

Molecular Alignment of Bulk Water: Observing a Giant THz Kerr Effect upon Librational Excitation

Fabio Novelli¹, Federico Sebastiani¹, Claudius Hoberg¹, Luis Ruiz Pestana^{3,4}, Kochise C. Bennett^{3,4}, Nikolas Stavrias², Lex A.F.G. Van Der Meer², Gerhard Schwaab¹, Teresa Head-Gordon^{3,4}, Martina Havenith^{1,*}

¹Lehrstuhl für Physikalische Chemie II, Ruhr-Universität Bochum, 44780 Bochum, Germany

²Radboud University, Institute for Molecules and Materials, FELIX Laboratory, Toernooiveld 7c, Nijmegen, Netherlands

³Chemical Sciences Division, Lawrence Berkeley National Laboratory

⁴Pitzer Center for Theoretical Chemistry, Departments of Chemistry, Chemical and Biomolecular Engineering, and Bioengineering, University of California, Berkeley, Berkeley, CA 94720

One Sentence Summary: We report experimental and theoretical evidence that THz excitation of the librational band results in efficient alignment of water molecules in the bulk

Abstract: Induced orientation of a molecule in real space by static and intense laser fields has been successfully employed to control reactions in the gas phase. However, for bulk water an effective alignment was not realized, yet due to the fast energy dissipation into the water network. Here we report a nonlinear Terahertz (THz) experiment carried out at the free electron laser FELIX. At 11.7 THz we observe a giant, resonance enhanced Kerr parameter which exceeds previous values by 4 orders of magnitude. Using ab initio molecular dynamics calculations, the large THz Kerr effect can be rationalized in terms of a linear response of a driven resonance orientation upon excitation of single water rotations. Our results suggest that bulk water can be efficiently aligned by THz laser fields around 12 THz.

*Correspondence to: martina.havenith@rub.de

The hindered librational motions of water molecules are of central importance for breaking and reforming hydrogen bonds(1), and are of particular significance to the diffusional process in liquid water(2). However, by exerting control on the molecular alignment using electric fields to create a preferred orientation of water dipoles, we could tune and control reactions in bulk solution. Although isolated molecules can be realigned if the electric field-dipole interaction exceeds the internal rotational energy(3–7), for liquid water the intermolecular interactions with the surrounding molecules introduces additional frictional forces that oppose an efficient global molecular alignment of water molecules by the electric field(8). In order to efficiently align the water molecules in the bulk liquid, the time scales of the light-triggered librational motion need to match the time scale of the reorientations of the surrounding “cage” molecules(9, 10).

Upon excitation of the librational mode in water, Hynes and co-workers observed an oscillation in the simulated energy on time scales of ~ 25 fs that is attributed to relaxation of rotational motions(8). The repulsive torques exerted by the hydrogen-bonded network cause a periodic oscillation of the strongly damped rotational motion of a single water molecule. As a consequence, the amount of energy transferred from the electric field to the central water molecule has a strong frequency dependence(8) that can be probed spectroscopically. For non-linear Kerr experiments, a linearly polarized pump field induces a birefringence Δn in the medium, which is monitored by a delayed probe pulse whose polarization is rotated by $\sim \pi/4$ to maximize the signal; given a pump intensity I , $\Delta n/I = n_2^l$ measures the birefringence which is proportional to the third-order susceptibility. While optical Kerr experiments probe the induced birefringence as an electronic response of the system(11), hybrid Terahertz (THz) Kerr experiments(9, 12–14) are more sensitive to nuclear dynamics. However, the reported hybrid THz-pump optical-probe Kerr parameters for liquid water(14) showed limited molecular alignment (Table S1).

THz light extends the dielectric regime from ns motions down to sub-ps time scales, i.e. the regime where librational, translational and other collective motions of the hydrogen-bonded water network come into play(15). However full THz pump-probe experiments are challenging due to the strong absorption of water and the scarce availability of high power sources(16–19).

We report THz pump – THz probe experiments at 11.7 THz and 7.8 THz in a Kerr geometry (Figure 1a) to selectively drive and align single molecule librations within the cage of the collective hydrogen-bonded network, thereby counteracting the ultrafast energy dissipation due to librational relaxation in the bulk liquid. In Figure 1b the polarization of the THz probe encloses an angle $\theta \sim \pi/4$ with respect to that of the linearly polarized THz pump field. We record the transmitted THz probe intensity along the pump direction as well as

perpendicular to it (Figure 1c for $\theta \sim 50^\circ$; Figure 1e for $\theta \sim 30^\circ$). At positive pump-probe delays, the probe polarization is expected to undergo both a Kerr ellipticity, $\epsilon(\theta, t)$, and an intensity change that depends on the time-dependent absorption $\Delta\alpha_{\parallel}(t)$ and $\Delta\alpha_{\perp}(t)$.

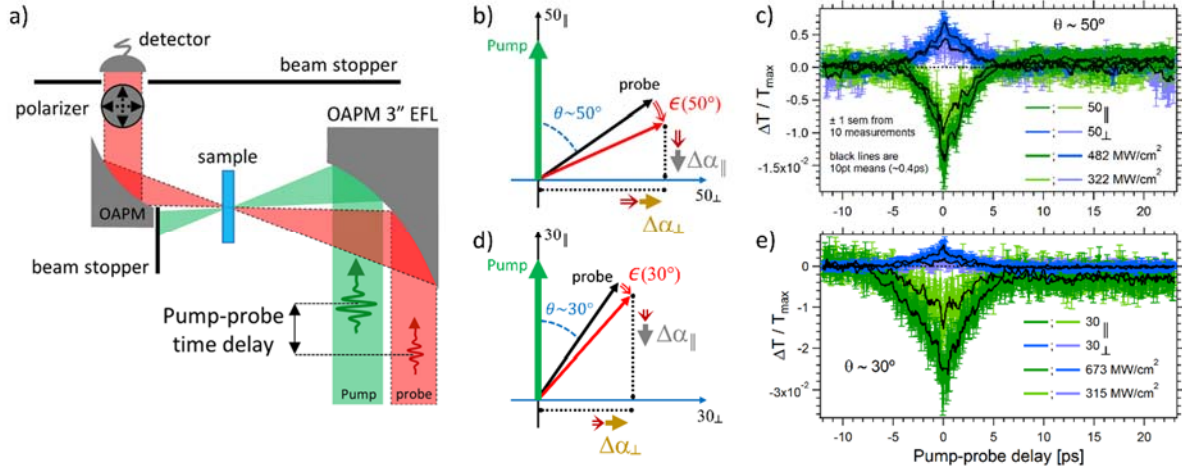


Figure 1. *Experimental configuration and Kerr transients in water.* (a) A 3” diameter off-axis parabolic mirror (PM) with 3” effective focal length focuses both pump and probe beams at the sample position. A second PM collects only radiation in the probe direction. The pump beam is vertically polarized and the probe beam is polarized at an angle θ before the sample. A second polarizer is placed before the detector. Several beam blockers minimize the pump scattering into the detector. (b-c) The probe is polarized at $\theta \sim 50^\circ$ with respect to the pump, (d-e) same as (b-c) except $\theta \sim 30^\circ$. (c,e) Pump-probe traces acquired at the different probe polarization angles, in direction parallel (green) and perpendicular (blue) to the pump polarization. Two pump intensities are shown for each experimental configuration, higher pump intensities are reported with darker colors and lower intensities in lighter shades. The measurements have been performed over different beamtimes and experimental conditions: pulse length is ~ 3 ps in panel (c) and ~ 4 ps in panel (e). Error bars are ± 1 standard errors of the mean from 10 measurements; black lines are the mobile average including 10 points over 0.4 ps.

At 11.7 THz we detect a clear signal at pump-probe overlap, spanning ~ 5 ps around pump-probe time $t = 0$. If the probe polarization is at an angle θ compared to the reference system, the intensity of the probe light transmitted parallel to the reference (θ_{\parallel}) is $T_{\parallel,eq} = e^{-\alpha d} \cos^2 \theta$, with α being the absorption coefficient at equilibrium and d sample thickness. By analogy, $T_{\perp,eq} = e^{-\alpha d} \sin^2 \theta$ is perpendicular to the reference (θ_{\perp}), and $T_{max} = e^{-\alpha d}$ along the probe direction. When the pump is turned on, we replace $\alpha \rightarrow \alpha + \Delta\alpha(t)$ and $\theta \rightarrow \theta + \epsilon(\theta, t)$. We acquire two pump-probe probe traces, along θ_{\parallel} and θ_{\perp} , corresponding to

$$\Delta T_{\perp}(\theta, t)/T_{max} = (T_{\perp}(t) - T_{\perp,eq})/T_{max} = [e^{-\Delta\alpha_{\perp}(t)d} \sin^2(\theta + \epsilon(\theta, t))] - \sin^2(\theta)$$

and

$$\Delta T_{\parallel}(\theta, t)/T_{max} = (T_{\parallel}(t) - T_{\parallel,eq})/T_{max} = [e^{-\Delta\alpha_{\parallel}(t)d} \cos^2(\theta + \epsilon(\theta, t))] - \cos^2(\theta)$$

For $\theta \sim \pi/4$ and $\epsilon, \Delta\alpha_{\parallel}d, \Delta\alpha_{\perp}d \ll 1$, we have $\Delta T_{\perp}/T_{max} \approx +\epsilon(\theta, t) - \Delta\alpha_{\perp}(t)d/2$ and $\Delta T_{\parallel}/T_{max} \approx -\epsilon(\theta, t) - \Delta\alpha_{\parallel}(t)d/2$. If the medium is transparent, $\Delta\alpha_{\parallel}(t) \approx \Delta\alpha_{\perp}(t) \approx 0$,

yielding the same equations as in Refs.(9, 12, 14). However, for all-THz Kerr, the two pump-probe traces have opposite sign but different magnitude, indicating that $\Delta\alpha_{\parallel}(t) \neq \Delta\alpha_{\perp}(t) \neq 0$. In the SI we determine $\Delta\alpha_{\parallel}(t)$, $\Delta\alpha_{\perp}(t)$, and $\epsilon(\theta, t)$, report additional pump-probe measurements, and show that all pump-probe signals scale with pump intensity (Figure S2). The obtained THz Kerr parameter for water, $n_2^I = (1 \pm 0.15) \cdot 10^{-11} \text{ cm}^2/\text{W}$, is $\sim 25000\times$ larger than those reported in optical and hybrid optical-THz Kerr experiments(14), and $\sim 200\times$ larger than the static Kerr(20) (Table S1).

The frequency-resolved signal, $S(\omega)$ probes the energy exchange between the field and water solvent defined in terms of the polarization and the probe field as

$$S(\omega) \propto \epsilon_S^*(\omega) \langle P(\omega) \rangle \sim \epsilon_S^*(\omega) \langle \vec{\mu}(\omega) \rangle \quad (2)$$

where ω is the detected frequency, $P(\omega)$ is the frequency-domain material polarization, and $\epsilon_S^*(\omega)$ is the negative frequency component of the probe field spectral envelope. Within the dipole approximation, the polarization P can be replaced by the material dipole $\vec{\mu}$ and a perturbative expansion results in a correlation function of dipole operators. The third-order Kerr process corresponds to a four-point time correlation function, however direct simulation of this quantity is prohibitively costly for all but the simplest systems(21). To gain insight into the rotational librational motions of water, we use *ab initio* molecular dynamics (AIMD) simulations to analyze $\dot{\theta}_i$, the rate of reorientation of the dipole $\vec{\mu}_i$ of molecule i with respect to the electric field \vec{E} , where $\theta_i = \angle(\vec{\mu}_i, \vec{E})$.

To identify the principal modes governing this rotational motion, we calculate the fast Fourier transform (FT) of the reorientation rate averaged over all the molecules (Figure 2a). It is evident that equilibrium fluctuations of single water molecules give rise to excitations that determine a maximum which is red-shifted compared to the maximum of the absorption. The linear response result reveals that the resonance frequency of the THz pump-probe experiments corresponds to the damped, single water molecule rotation at ~ 14 THz(22–24). The fluctuation-dissipation process is shown in Figure 2b when a strong static field of 25.7 MV/cm is applied at trajectory time 0 and turned off at 0.5 ps. At $t = 0$ ps and $t = 1$ ps no net orientation can be observed, indicating that water relaxes with a time constant of $t_{relax} = 0.5$ ps. Thus the equilibrium fluctuations of the single molecule rotations within the "cage" of the collective hydrogen-bonded network result in a rapid dissipation of rotational coherence. This agrees with the experimental results (Figure 1), where signal can be observed only at pump-probe overlap, which is much longer than t_{relax} .

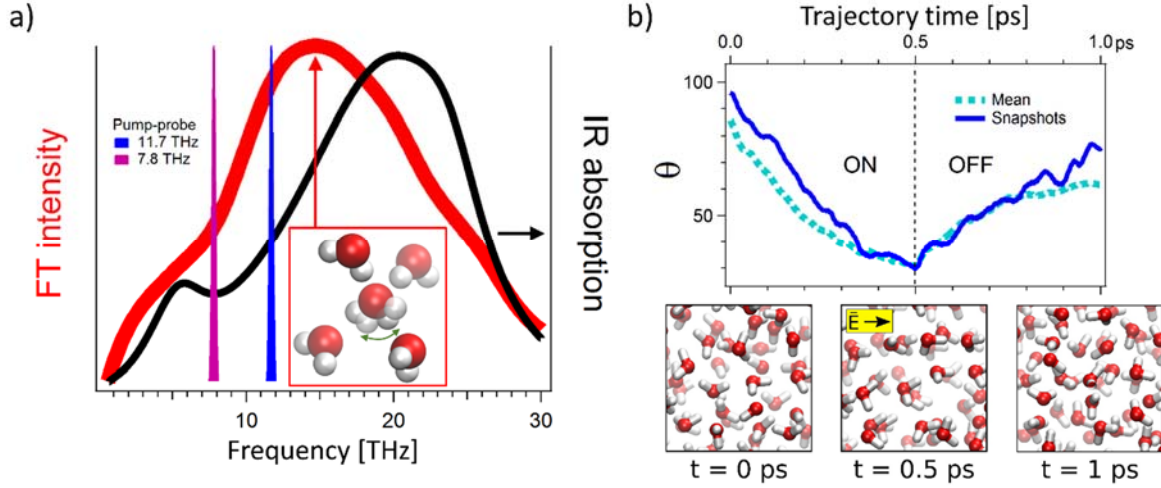


Figure 2. Fluctuation-dissipation results for rotational relaxation in the bulk water solvent. (a) The absorption coefficient of water(22) (black) and the FT of the reorientation rate (red) are plotted versus frequency. The experimental pulses are shown, together with a sketch of the single water molecule libration in a cage of nearest neighbors (inset). (b) AIMD calculations showing the recovery of the single-molecule water dynamics below the experimental resolution, i.e. on a ~ 0.5 ps timescale. Here a static electric field of amplitude 25.7 MV/cm is turned on at time zero and turned off at 0.5 ps. The molecular arrangements at $t=0, 0.5, 1$ ps are shown in panels on the bottom right.

The pump-probe trace perpendicular to the pump direction $\Delta T_{\perp}(\theta \sim \pi/4, t)/T_{max} \approx +\epsilon(\theta, t) - \Delta\alpha_{\perp}(t)d/2$ is large and positive and can be used to measure the magnitude of the Kerr effect. In Figure 3a we compare the Kerr fingerprint trace $\Delta T_{\perp}(\theta = 30^{\circ}, t)/T_{max}$ for pump pulses at 11.7 THz (blue, from Figure 1e) and 7.8 THz (purple). At 7.8 THz we detect no Kerr signal within the experimental uncertainty.

To simulate the Kerr effect at the two frequencies, we approximate the nonlinear third-order Kerr effect by taking the difference between the time-dependent simulation of the molecular dynamics in the presence of a pump field to provide the full signal $S(\omega)$ and an expectation value over the unpumped state that yields the ordinary absorption, $S_0(\omega)$. We apply a square wave pump field and propagate in real time using AIMD to obtain a time series of dipoles that can be FFT to obtain the $S(\omega)$ spectrum. The difference quantity

$$\Delta = S(\omega) - S_0(\omega) \sim \epsilon_S^*(\omega) [\langle \vec{\mu}(\omega) \rangle - \langle \vec{\mu}(\omega) \rangle_0] \quad (3)$$

as a function of the ω_{pump} is plotted in Figure 3b for the bulk water system.

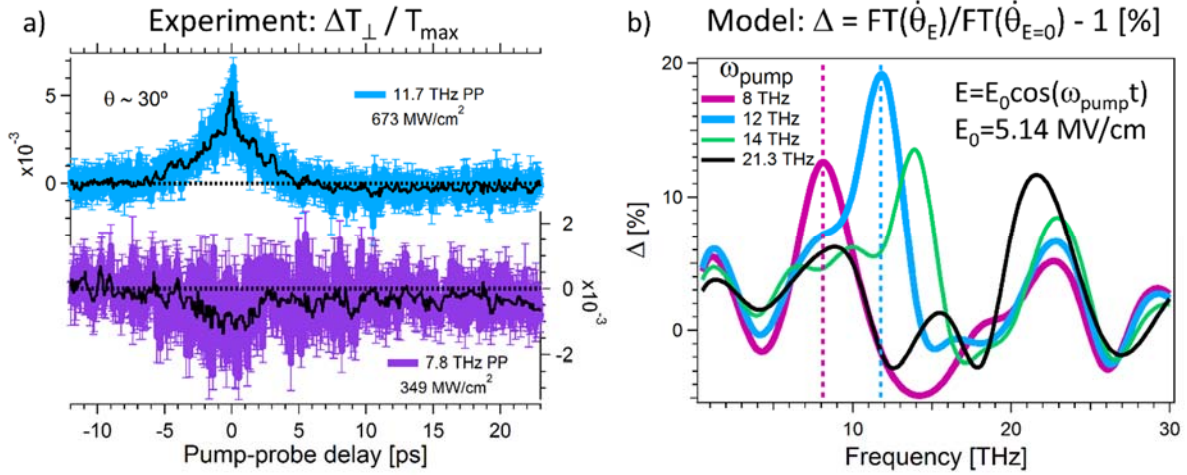


Figure 3. Frequency-dependent Kerr effect and simulated spectrum. (a) Measured pump-probe traces perpendicular to the pump direction in water for 11.7 THz (blue) and 7.8 THz pulses (purple). No Kerr signal can be found at 7.8 THz. (b) Simulated response of bulk water to an applied AC field $E \approx E_0 \cos(\omega_{\text{pump}} t)$ lasting 0.5 ps, with frequency $\omega_{\text{pump}} = 8, 12, 14,$ and 21.3 THz, and an amplitude $E_0 = 5.14 \text{ MV/cm}$. As the field frequency is varied from 8 THz to 21.3 THz, a resonant effect appears: the reorientation is maximum at 12 THz and lower at 8 THz, in qualitative agreement with the experimental results.

Figure 3 shows that the bulk water alignment effect is found to be both frequency and field dependent. Large fields ($E_0 = 25.7 \text{ MV/cm}$) drive the system too hard and saturates the response regardless of ω_{pump} while for much lower fields no significant Kerr effect is evident (Figure S3). For amplitude $E_0 = 5.14 \text{ MV/cm}$ the dipole alignment relaxation is strongly frequency dependent and most pronounced at 12 THz, in striking agreement with the experiment. At 12 THz, the driving and relaxation processes are on the same timescale as the natural fluctuations of the system, leading to rapid and efficient orientational alignment. When ω_{pump} is lowered to 8 THz, less energy is deposited into the system because of the lower absorption coefficient and, most importantly, the timescale of the driving field is detuned with respect to natural system fluctuations, resulting in less efficient molecular alignment.

The giant magnitude of the Kerr signal at 11.7 THz in water can be explained by a resonance effect(8, 21, 25, 26) which matches the single molecules reorientational time in the bulk phase at equilibrium. While the molecular alignment is reminiscent of a preferred orientation of water dipoles in e.g. membrane channels, in graphene layers or, more in general, under confinement(27, 28), our results now pave the way to tune and control reactions even in bulk solutions by tailoring the properties of driving THz fields.

Acknowledgments. The authors acknowledge S. Schäfer, B. Redlich, K. Saeedi Ilkhchy, and V. Eless for experimental support. We thank the Cluster of Excellence RESOLV (EXC 1069), ERC Advanced Grant 695437, LASERLAB-EUROPE grant 654148 for financial support.

Berkeley thanks the U.S. DOE under Contract No. DE-AC02-05CH11231. K.C.B. thanks the California Alliance Postdoctoral Fellowship and T. H.-G. for support as a RESOLV Fellow.

1. A. Luzar, Resolving the hydrogen bond dynamics conundrum. *J. Chem. Phys.* **113**, 10663–10675 (2000).
2. D. Laage, J. T. Hynes, A molecular jump mechanism of water reorientation. *Science*. **311**, 832–5 (2006).
3. B. Friedrich, D. Herschbach, Manipulating molecules via combined static and laser fields. *J. Phys. Chem. A*. **103**, 10280–10288 (1999).
4. B. Friedrich, D. Herschbach, Alignment and Trapping of Molecules in Intense Laser Fields. *Phys. Rev. Lett.* **74**, 4623–4626 (1995).
5. E. W. Kuipers, M. G. Tenner, A. W. Kleyn, S. Stolte, Observation of steric effects in gas–surface scattering. *Nature*. **334**, 420–422 (1988).
6. S. Fleischer, Y. Zhou, R. W. Field, K. A. Nelson, Molecular Orientation and Alignment by Intense Single-Cycle THz Pulses. *Phys. Rev. Lett.* **107**, 163603 (2011).
7. S. Fleischer, R. W. Field, K. A. Nelson, Commensurate two-quantum coherences induced by time-delayed THz fields. *Phys. Rev. Lett.* **109**, 1–5 (2012).
8. J. Petersen, K. B. Møller, R. Rey, J. T. Hynes, Ultrafast librational relaxation of H₂O in liquid water. *J. Phys. Chem. B*. **117**, 4541–4552 (2013).
9. M. Sajadi, M. Wolf, T. Kampfrath, Transient birefringence of liquids induced by terahertz electric-field torque on permanent molecular dipoles. *Nat. Commun.* **8**, 14963 (2017).
10. F. W. Deeg, J. J. Stankus, S. R. Greenfield, V. J. Newell, M. D. Fayer, Anisotropic reorientational relaxation of biphenyl: Transient grating optical Kerr effect measurements. *J. Chem. Phys.* **90**, 6893–6902 (1989).
11. A. Taschin, P. Bartolini, R. Eramo, R. Righini, R. Torre, Evidence of two distinct local structures of water from ambient to supercooled conditions. *Nat. Commun.* **4**, 1–8 (2013).
12. M. C. Hoffmann, N. C. Brandt, H. Y. Hwang, K.-L. Yeh, K. A. Nelson, Terahertz Kerr effect. *Appl. Phys. Lett.* **95**, 231105 (2009).
13. I. A. Finneran, R. Welsch, M. A. Allodi, T. F. Miller, G. A. Blake, Coherent two-dimensional terahertz-terahertz-Raman spectroscopy. *Proc. Natl. Acad. Sci.* **113**, 6857–6861 (2016).
14. P. Zalden *et al.*, Molecular polarizability anisotropy of liquid water revealed by terahertz-induced transient orientation. *Nat. Commun.* **9**, 2142 (2018).
15. M. Heyden *et al.*, Dissecting the THz spectrum of liquid water from first principles via correlations in time and space. *Proc. Natl. Acad. Sci.* **107**, 12068–12073 (2010).
16. M. Shalaby, C. P. Hauri, Demonstration of a low-frequency three-dimensional terahertz bullet with extreme brightness. *Nat. Commun.* **6**, 5976 (2015).

17. M. Knorr *et al.*, Phase-locked multi-terahertz electric fields exceeding 13 MV/cm at a 190 kHz repetition rate. *Opt. Lett.* **42**, 4367 (2017).
18. B. Liu *et al.*, Generation of narrowband, high-intensity, carrier-envelope phase-stable pulses tunable between 4 and 18 THz. *Opt. Lett.* **42**, 129 (2017).
19. T. I. Oh *et al.*, Intense terahertz generation in two-color laser filamentation: energy scaling with terawatt laser systems. *New J. Phys.* **15**, 075002 (2013).
20. B. M. Novac *et al.*, Determination of the Kerr Constant of Water at 658 nm for Pulsed Intense Electric Fields. *IEEE Trans. Plasma Sci.* **40**, 2480–2490 (2012).
21. T. Yagasaki, S. Saito, Ultrafast intermolecular dynamics of liquid water: A theoretical study on two-dimensional infrared spectroscopy. *J. Chem. Phys.* **128**, 154521 (2008).
22. H. R. Zelsmann, Temperature dependence of the optical constants for liquid H₂O and D₂O in the far IR region. *J. Mol. Struct.* **350**, 95–114 (1995).
23. D. C. Elton, M. Fernández-Serra, The hydrogen-bond network of water supports propagating optical phonon-like modes. *Nat. Commun.* **7**, 1–8 (2016).
24. P. Schienbein, G. Schwaab, H. Forbert, M. Havenith, D. Marx, Correlations in the Solute-Solvent Dynamics Reach beyond the First Hydration Shell of Ions. *J. Phys. Chem. Lett.* **8**, 2373–2380 (2017).
25. R. Rey, J. T. Hynes, Solvation Dynamics in Liquid Water. III. Energy Fluxes and Structural Changes. *J. Phys. Chem. B.* **121**, 1377–1385 (2017).
26. F. Ingrosso, R. Rey, T. Elsaesser, J. T. Hynes, Ultrafast Energy Transfer from the Intramolecular Bending Vibration to Librations in Liquid Water. *J. Phys. Chem. A.* **113**, 6657–6665 (2009).
27. D. Muñoz-Santiburcio, D. Marx, Nanoconfinement in Slit Pores Enhances Water Self-Dissociation. *Phys. Rev. Lett.* **119**, 056002 (2017).
28. V. V. Welborn, L. R. Pestana, T. Head-Gordon, Computational Optimization of Electric Fields for Better Catalysis Design (Perspective - in press). *Nat. Catal.* (2018).